Science Article

Climate model simulations of the meteorological effects of superflare events

Tammas F. Loughran and Kevin J. E. Walsh

School of Earth Sciences, University of Melbourne, Parkville, Victoria

Address for correspondence: tammasfl@unimelb.edu.au

1. Introduction

Flare events are common on the Sun and are sometimes associated with magnetic storms on Earth that cause havoc with our communication systems, satellites and power grids. However, observed solar flares pale in comparison to the events that can occur on other stars, where short duration events known as superflares release total energies of at least 10^{25} J. This is 100 times larger than the largest known event on the Sun—the Carrington event of 1859 (Tsurutani et al., 2003). They are thought to be caused by a similar mechanism to solar flares (Schaefer, 1989) and can occur on many different star types including those similar to the Sun (Schaefer et al., 2000). Since flares are caused by strong magnetic fields in the Sun's atmosphere, observations of sunspots, and therefore the associated magnetic activity, indicate that superflares are unlikely to have occurred on the Sun in the last 400 years (Schrijver et al., 2012). Nevertheless, there exists evidence that there have been very large cosmic events in Earth's history (Miyake et al., 2012) and a superflare is a good candidate for their origin (Melott and Thomas, 2012).

Maehara et al., (2012) used observations of superflares from the Kepler telescope to estimate the frequency of a flare with a total energy of 10^{27} J on Sun-like stars to be about once every 800 years. Although it is unlikely, the possibility that the Sun will suffer a superflare is not zero. A superflare event could be devastating to modern society but the effects of such a flare on Earth's weather have not yet been evaluated. In addition, what might a superflare imply for the habitability and likelihood of life on other Earth-like planets? In this study a climate model will be used to investigate the effects that radiation from a superflare would have on the weather and climate of Earth and Earth-like planets.

2. Calculating the Solar flux at Earth's distance

A method for calculating the evolution of radiation at the top of the atmosphere during a superflare is first developed. Here we follow Schaefer et al., (2000) who compiled a list of superflares that have been observed on G-type main sequence stars[1]. Their total energies range from 10^{26} J to 10^{31} J and their durations range from minutes to days. Maehara et al., (2012) also compiled a database of superflare observations on G-type main sequence stars from the Kepler satellite where it can be seen that the energy emission of a superflare is characterised by a sudden increase in brightness followed by a gradual decrease.

Based on these observations we can approximate the evolution of the power output with a simple function (Eq. 1) that displays the observed behaviour. *P(t)* is the power output of the flare in watts at time *t*. *A* is a scaling factor that controls the amplitude of the flare and *B* is a scaling factor that controls the time of maximum output of the flare. *E* (Eq. 2) is the total energy emitted by the flare and can be found as the integral of (1) over the duration of the flare, *D*, in seconds. Solving this integral yields equation (3). Finally, substituting (3) into (1) results in an expression for the power of the flare (4).

$$P(t) = \frac{A}{B} t e^{\frac{-t}{B}} \tag{1}$$

$$E = \int_0^D P(t)dt \tag{2}$$

$$E = A(-e^{\frac{-D}{B}}(B + D) + B) \tag{3}$$

$$P(t) = \frac{E}{B(-e^{\frac{-D}{B}}(B + D) + B)} t e^{\frac{-t}{B}} \tag{4}$$

The evolution of the flare output asymptotes to zero, so it must be truncated at the end of a specified duration. If the maximum is specified to be too late in the flare then the flare will end abruptly, which is uncharacteristic of the observations. In this study, *B* is defined as one ninth of the duration of the flare. Given that we know the total energy output of a superflare and its duration, we can then calculate an approximation of its evolution.

---

[1]   A main sequence star is a star that uses hydrogen as its main fuel for nuclear fusion. The Sun is one example of a G-type main sequence star.

Star	Energy (J)	D (sec)	$\Delta W(B)$ (Wm^{-2})
Gmb 1830	1.00×10^{28}	1030	220.33
k Ceti	2.00×10^{27}	2400	19.83
MT Tau	1.00×10^{28}	600	386.00
Pi Uma	2.00×10^{26}	2100	2.26
S For	2.00×10^{31}	1120	466585.30
BD + 10	3.00×10^{27}	2940	24.28
o Aql	9.00×10^{29}	432000	49.57
5 Ser	7.00×10^{30}	259200	642.63
UU CrB	7.00×10^{28}	3420	487.05

Table 1: A list of superflares from Schaefer et al. (2000), including S Fornacis, with their total energies, durations D and the maximum anomalous radiation flux at the top of the atmosphere ΔW(B).

The next step is to calculate the resulting radiation flux at the Earth. In order to simplify the problem, we have assumed that the flare occurs at the closest point on the Sun to the Earth and is directed straight at the Earth. The inverse square rule is used to calculate the flux from the flare ($\Delta W(t)$) over a hemisphere with a radius that spans the distance from the flare to the Earth (e.g. Eq. 5), where r is the mean Earth-Sun distance and R is the radius of the Sun. The total flux at the top of the atmosphere would therefore be the regular solar constant (1365 Wm^{-2}) plus the flux from the flare.

$$\Delta W(t) = \frac{P(t)}{2\pi(r-R)^2} \qquad (5)$$

Table 1 lists some examples of the maximum anomalous radiation at the top of the atmosphere ($\Delta W(B)$) during a superflare for planets that are 1 AU (Earth-Sun distance) from their star. Most of the values of $\Delta W(B)$ are small compared with the average solar constant for Earth. It is expected that these flares would be too weak to have any significant radiative impact on the Earth's atmosphere. The exception to this is the S Fornacis (S For) flare which is several orders of magnitude greater than other observed flares. Due to uncertainty in the observed duration of the S For flare, the longest possible duration is six hours giving
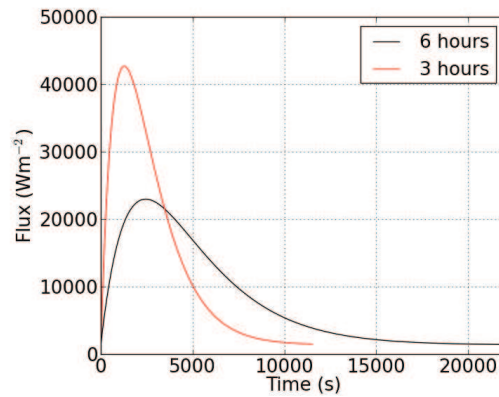

Figure 1: Time evolution of top of the atmosphere incoming solar radiation of S Fornacis superflares assuming 3.5 hours and 6 hours duration at 1 AU from the Sun.

a maximum flux of 22978 Wm^{-2}, which is more than 16 times the solar constant. That is, longer flares of the same energy have lower maximum output as shown in Figure 1.

3. Model

For this study we are using the CSIRO Mk3L climate model (Phipps et al., 2011) to simulate a planet identical to Earth. It is a fully coupled atmosphere, land, sea ice and ocean general circulation model (GCM). The atmosphere has a coarse spectral resolution of R21 corresponding to 5.625° longitude by ~3.18° latitude grid spacing with 18 hybrid vertical levels. It features a prognostic stratiform cloud scheme (Rotstayn, 1997) as well as the U.K. Meteorological Office convective cloud scheme (Gregory and Rowntree, 1990).

At the start of each simulation, the energy and duration of the flare is specified and an appropriate insolation profile is calculated. A superflare is represented within the model by modifying the solar constant at each time step. Of the superflares from Table 1, three were selected to represent a range of flares that might have a noticeable impact on Earth or an Earth-like planet: the S For flare with a duration of six hours, the 5 Serpentis (5 Ser) flare with a duration of three days and the o Aquilae (o Aql) flare with a duration of five days. For each flare, a simulation was

Month	January	June
	Control	Control
Simulation	S Fornacis (S For)	S Fornacis (S For)
	o Aquilae (o Aql)	o Aquilae (o Aql)
	5 Serpentis (5 Ser)	5 Serpentis (5 Ser)

Table 2: A list of simulations for the January and July experiment. Control simulations involve no flare event.

Region	Australia	South America	Pacific Ocean	Asia
Simulation	Control	Control	Control	Control
	S Fornacis	S Fornacis	S Fornacis	S Fornacis

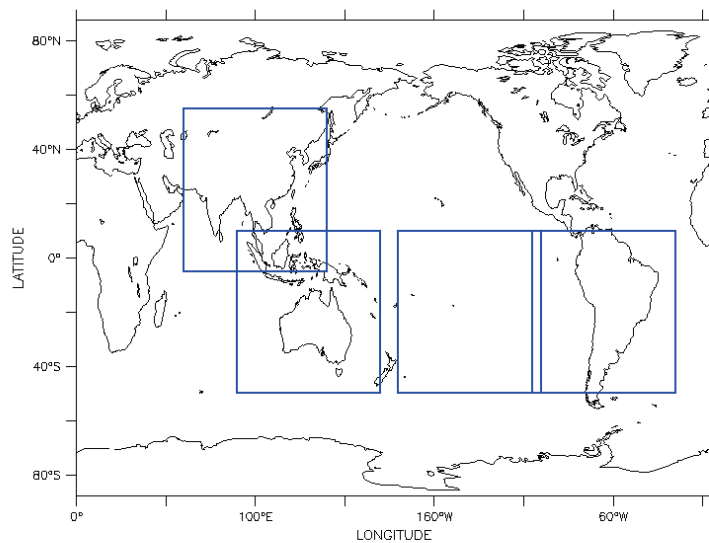Table 3: A list of simulations for the positioned flares experiment.

Figure 2: Averaging regions for positioned S For superflares. Australia (10°N–50°S, 90°E–170°E), Pacific (10°N–50°S, 180°E–260°E), South America (10°N–50°S, 255°E–355°E) and Asia (55°N–5°S, 60°E–140°E).

run in January and June (listed in Table 2) to determine if there would be any differences in the effects of the flare between the Northern and Southern Hemispheres.

The region exposed to the longer duration flares spans almost the entire globe, but the S For flare would only affect particular regions because it lasts six hours. Therefore, to examine the effect of a superflare on continental and oceanic regions, the S For simulations were repeated with the flare positioned over the regions listed in Table 3 with maximum insolation occurring at the centre of the boxes in Figure 2. Flares were positioned over Australia, South America, the Pacific Ocean (all occurring in January) and Asia (occurring in June) (see Figure 2).

4. Results

4.1 January and June flares

For the flares in January and June, the grid point maximum surface temperatures reached during each superflare are presented in Table 4 as well as the grid point maximum sea surface temperatures (SSTs) over the duration of the flare. The longer duration flares o Aql and 5 Ser give temperatures only 2.7°C and 5.7°C (respectively) higher than the control simulations. The S For flare, on the other hand, resulted in surface temperature maxima of 201°C in June and 188°C in January. The 201°C from the June simulation is an unusually high value compared to its surrounding grid points, suggesting a possible over

estimate by the model. However, there are several other instances of surface temperatures of up to 140°C in this simulation which may be a more realistic response.

In contrast, maximum SSTs remained unchanged for the long duration flares. Only the S For flare causes any noticeable difference in SST from the control. For this flare, the thermal response in June is slightly larger than that in January.

4.2 Positioned flares

Flares positioned over continents produced the most extreme temperatures. Table 5 shows the maximum grid point surface temperatures reached for each region. Surface temperatures for the flares positioned over continents reach 202°C but there was little difference between them due to surface energy balance conditions. The flare positioned over the Pacific caused surface temperatures to reach 109°C and occurred at the nearest land point which was the west coast of South America.

There were large changes to clouds and rainfall during the flares. Firstly, the total cloud coverage decreased over oceans. Figure 3a shows the difference in cloud cover fraction between the control simulation and the S For flare simulation positioned over Australia. The flare simulation was dominated by a decrease in cloudiness over the ocean while the only cloud development occurred over land. Secondly, rain was also suppressed over the ocean but the

	Max. surface temp. (°C)		Max. SST(°C)	
	January	June	January	June
Control	55.75	59.45	29.4554	30.4985
o Aql	58.35	58.45	29.5149	30.503
5 Ser	59.45	65.15	29.5385	30.568
S For	188.49	201.05	30.491	30.974

Table 4: Gridpoint maximum surface temperature and maximum sea surface temperature for each flare in January and June.

Simulation	Max. surface temp. (°C)
January control	55.65
June control	59.25
Pacific	110.65
Australia	203.75
South America	203.45
Asia	203.25

Table 5: Grid point maximum surface temperature for flares positioned over each region during the S Fornacis simulations and control simulations.
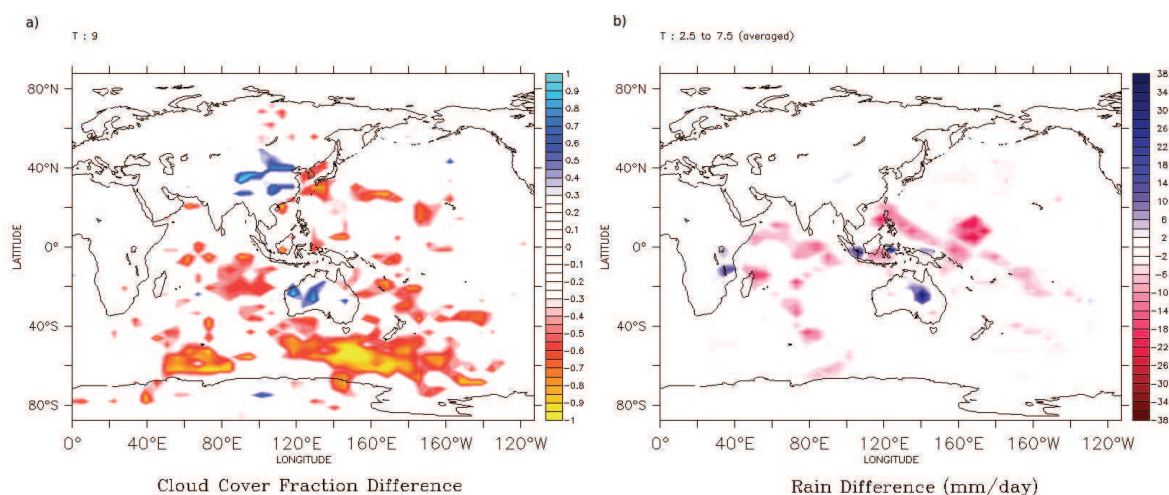
Figure 3: (a) Cloud cover fraction difference between the S For flare and control simulations positioned over Australia and (b) the same for rainfall intensity averaged over the duration of the flare. Negative values indicate a decrease in cloud or rain in response to the flare.
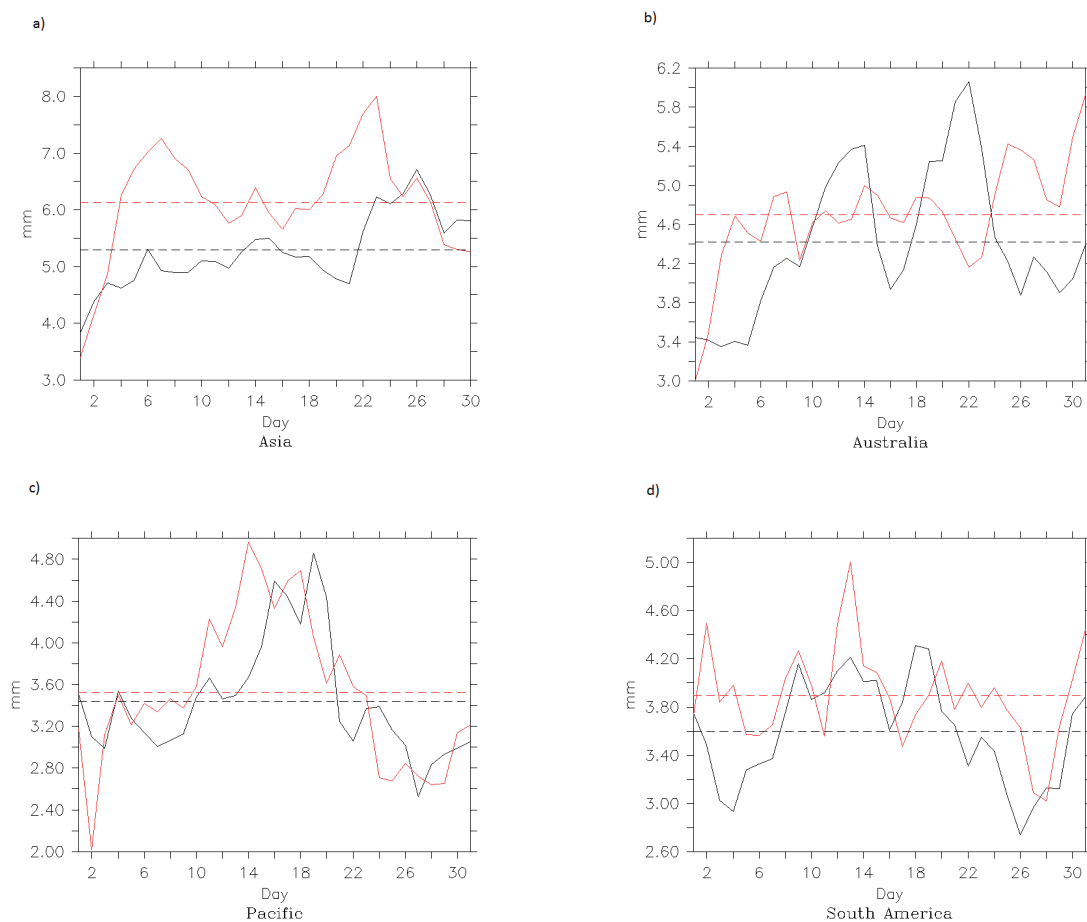

Figure 4: Time series of daily rain for up to one month after the S Fornacis superflare positioned over (a) Asia, (b) Australia, (c) Pacific Ocean, and (d) South America. The red lines are the flare simulations and the black lines are the control simulations. The horizontal dashed lines are the averages for the corresponding series.
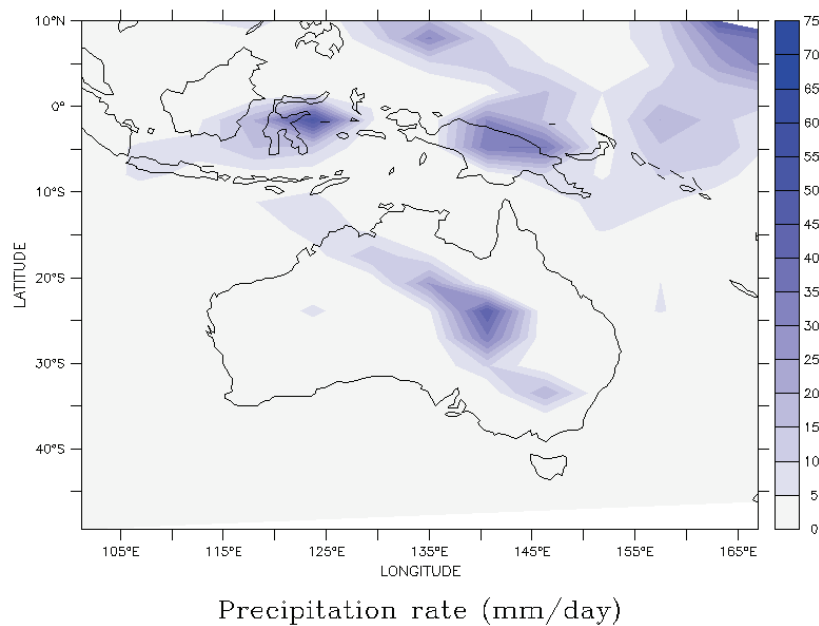
Precipitation rate (mm/day)

Figure 5: Rain intensity in the control simulation at 05:00 UTC (corresponding with the time the S For flare is positioned over Australia).

major rainfall increases occurred over land in Queensland and Indonesia (Figure 3b). Other flare simulations showed a similar behaviour for their respective regions (not shown).

In order to observe the longer-term effects of the S For flare on a particular region, average daily rainfall was calculated over the boxes in Figure 2. Figure 4 shows time series of total daily rainfall for each box for the control and flare simulations as well as the corresponding means. The means of daily rain for superflare simulations are greater than the control simulations, therefore a greater amount of rain fell in the weeks following a superflare. Unlike the continental simulations, rainfall in the Pacific simulation

is only slightly greater than its control simulation. This suggests that the presence of land is important for triggering convection and enhancing rainfall due to a superflare.

5. Discussion and Conclusion

The S For flare is much more powerful than the others due to its higher energy and shorter duration. Its short duration also means that the affected area is much smaller. The difference between June and January SST is due to the maximum insolation being located in the North West Pacific Ocean in June and Australia in January. The o Aql and 5 Ser flares are five and three days in duration
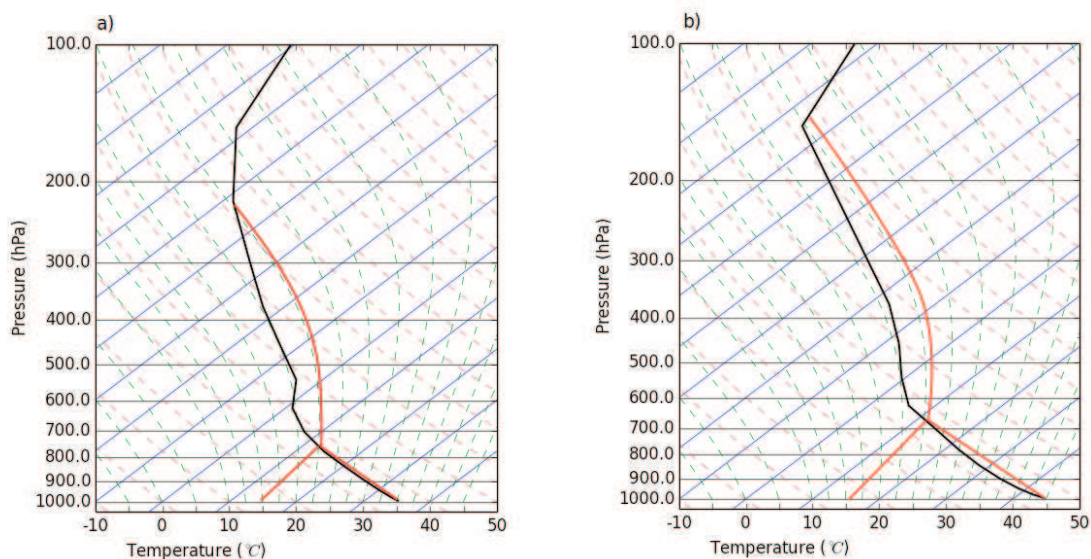

Figure 6: Vertical temperature profiles of the storm located at 140°E, 30°S for (a) the control simulation and (b) the S For superflare positioned over Australia. Both profiles are taken at the time of maximum insolation in the S For simulation. Black indicates the temperature profile and red indicates the 1000 hPa parcel trajectory. Land surface temperature has not been plotted here.

respectively and their effect is therefore distributed over most of the surface area of the globe.

Since there was little difference in maximum surface temperature between continents, the size of a landmass seems unimportant for extremes in temperature. Whether or not the superflare was positioned over a landmass, and not the size of the landmass, determined the maximum temperatures.

The decrease in cloud and rain during the flare could be due to accelerated evaporation of clouds in the model due to increased radiation. Intensification of storm systems only occurred where there was some pre-existing storm that had a large amount of available moisture. For example, a storm located over Australia in the control simulation (Figure 5) increased in intensity in response to the flare in the Australian S For simulation. Increases in rain intensity during the flare were seen in all S For simulations but only over land, whereby high temperatures created a large amount of CAPE-driven convection. Figure 6 shows the vertical temperature profiles of the storm from Figure 5 for the control and superflare simulations at the time of maximum insolation in the flare simulation. The surface based CAPE for this storm was 1575 J kg^{-1} for the control simulation and 2242 J kg^{-1} in the superflare simulation. In contrast to the land, it is hypothesised that temperatures over the ocean could not generate enough latent heat flux from the surface to overcome flare-induced evaporation of the clouds.

For Sun-like stars, the frequency of superflare events has been shown to obey a power law with higher energy flares being the rarest (Maehara et al., 2012). Therefore, it is expected that the S For flare is an extremely unusual event that is not likely to occur on the Sun. However, due to the small number of observations of superflares on Sun-like stars, there is large uncertainty in the frequency in high energy flares. The exact mechanism that causes superflares and whether or not they occur on the Sun is also still a topic of debate. If the Sun can create superflares, we have found that most flares would have little effect on the weather of a planet identical to Earth, except the highest energy short duration flares, such as S For. The surface temperature of 200°C produced by this flare is more than enough to cause widespread extinction of land based life but its short duration means that only about half of the planet's surface is exposed to it. Therefore, a large superflare event such as this may cause an extinction event similar to those experienced throughout Earth's history (e.g. Bambach et al., 2004) in which not all life would be affected. For planets that rotate as fast as Earth, only the global land surface exposed to the S For flare would experience such high temperatures. The o Aql and 5 Ser flares are very high energy flares in their own right but due to their long duration, similar flares would be unlikely to have any serious thermal effects on Earth's weather or climate.

References

Bambach, R.K., Knoll, A.H. and Wang, S.C., 2004, Origination, extinction, and mass depletions of marine diversity, *Paleobiology*, 30, 522–542.

Gregory, D. and Rowntree, P.R., 1990, A mass flux convection scheme with representation of cloud ensemble characteristics and stability-dependent closure, *Monthly Weather Review*, 118, 1483–1506.

Maehara, H., Shibayama, T., Notsu, S., Notsu, S., Nagao, T., Kusaba, S., Honda, S., Nogami, D. and Shibata, K., 2012, Superflares on solar-type stars, *Nature*, 485, 478–481.

Melott, A.L. and Thomas, B.C., 2012, Causes of an AD 774–775 14C increase, *Nature*, 491, doi:10.1038/nature11695.

Miyake, F., Nagaya, K., Masuda, K., and Nakamura, T., 2012, A signature of cosmic-ray increase in AD 774–775 from tree rings in Japan, *Nature*, 486, 240–242.

Phipps, S.J., Rotstayn, L.D., Gordon, H.B., Roberts, J.L., Hirst, A.C. and Budd, W.F., 2011, The CSIRO Mk3L climate system model version 1.0 – Part 1: Description and evaluation, *Geoscientific Model Development*, 4, 483–509.

Rotstayn, L.D., 1997, A physically based scheme for the treatment of stratiform clouds and precipitation in large-scale models: 1. Description and evaluation of the microphysical processes, *Quarterly Journal of the Royal Meteorological Society*, 123, 1227–1282.

Schaefer, B.E., 1989, Flashes from normal stars, *Astrophysical Journal*, 337, 927–933.

Schaefer, B.E., King, J.R. and Deliyannis, C.P., 2000, Superflares on ordinary solar-type stars, *Astrophysical Journal*, 529, 1026–1030.

Schrijver, C.J., Beer, J., Baltensperger, U., Cliver, E.W., Guedel, M., Hudson, H.S., McCracken, K.G., Osten, R.A., Peter, T.H., Soderblom, D.R., Usoskin, I.G. and Wolff, E.W., 2012, Estimating the frequency of extremely energetic solar events based on solar, stellar, lunar, and terrestrial records, *Journal of Geophysical Research: Space Physics*, 117, doi:10.1029/2012JA017706.

Tsurutani, B.T., Gonzalez, W,D., Lakhina, G.S. and Alex, S., 2003, The extreme magnetic storm of 1–2 September 1859, *Journal of Geophysical Research*, 108, doi:10.1029/2002JA009504.